

SpinalNet: Deep Neural Network with Gradual Input

H M Dipu Kabir, Moloud Abdar, Seyed Mohammad Jafar Jalali, Abbas Khosravi, Member, IEEE;
Amir F Atiya, Senior Member, IEEE; Saeid Nahavandi, Dipti Srinivasan, Fellow, IEEE.

Abstract—Deep neural networks (DNNs) have achieved the state of the art performance in numerous fields. However, DNNs need high computation times, and people always expect better performance with lower computation. Therefore, we study the human somatosensory system and design a neural network (SpinalNet) to achieve higher accuracy with lower computation time. This paper aims to present the SpinalNet. Hidden layers of the proposed SpinalNet consist of three parts: 1) Input row, 2) Intermediate row, and 3) output row. The intermediate row of the SpinalNet usually contains a small number of neurons. Input segmentation enables each hidden layer to receive a part of the input and outputs of the previous layer. Therefore, the number of incoming weights in a hidden layer is significantly lower than traditional DNNs. As the network directly contributes to outputs in each layer, the vanishing gradient problem of DNN does not exist. We integrate the SpinalNet as the fully-connected layer of the convolutional neural network (CNN), residual neural network (ResNet), and Dense Convolutional Network (DenseNet), Visual Geometry Group (VGG) network. We observe a significant error reduction with lower computation in most situations. We have received state-of-the-art performance for the QMNIST, Kuzushiji-MNIST, and EMNIST(digits) datasets. Scripts of the proposed SpinalNet is available at the following link: <https://github.com/dipuk0506/SpinalNet>

Index Terms—DNN, CNN, AdaNet, ResNet, DenseNet.

I. INTRODUCTION

Deep Neural Networks (DNNs) have brought the state of the art performance in various scientific and engineering fields [1]–[4]. DNNs usually have a large number of input features, as the consideration of more parameters usually improves the accuracy of the prediction. The size of the first hidden layer is critical. A small first hidden layer fails to propagate all input features properly while a large first hidden layer increases the number of weight drastically. Another limitation of the traditional DNNs is the vanishing gradient. When the number of layers is large, the gradient is high at neurons near output, and the gradient becomes negligible at neurons near inputs. DNN training becomes difficult due to the vanishing gradient problem.

The human brain is also receiving a lot of information from our skin. Numerous tactile sensory neurons are spread

H M Dipu Kabir, Moloud Abdar, Seyed Mohammad Jafar Jalali, Abbas Khosravi, and Saeid Nahavandi are with Institute for Intelligent Systems Research and Innovation (IISRI), Deakin University, Australia. (Email: {hussain.kabir, mabdar, sjalali, abbas.khosravi, saeid.nahavandi}@deakin.edu.au)

Amir F Atiya is with Cairo University. Email: amir@alumni.caltech.edu
Dipti Srinivasan is with National University of Singapore. Email: dipti@nus.edu.sg

Manuscript received –, 2020;
accepted—.

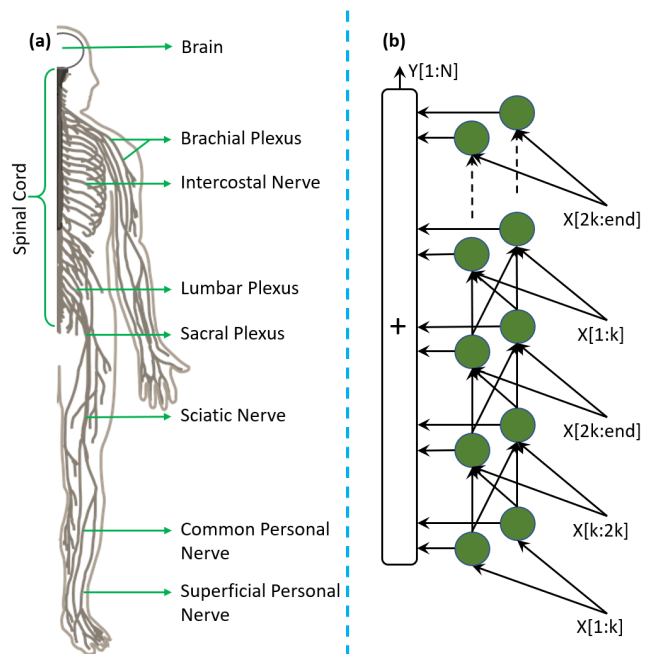


Fig. 1. The SpinalNet tries to mimic the human somatosensory system to receive large data efficiently and to achieve better performance. (a) Half part of the human somatosensory system, presenting how our spinal cord receives sensory signals from our body. (b) Structure of the proposed SpinalNet. The proposed NN consists of the input row, the intermediate row, and the output row. The intermediate row contains multiple hidden layers. Each hidden layer receives a portion of the input. All layers except the first layer also receive outputs of the previous layer. The output layer adds the weighted outputs of all hidden neurons of the intermediate row. The user can also construct and train a SpinalNet for any arbitrary number of inputs, intermediate neurons, and outputs.

throughout our bodies. They can sense pressure, heat, vibrations, complex textures, hardness, state of matter, etc. [5]. Humans can have different touch sensitivity over time. Although the exact mechanism is not unknown to humans, the current knowledge base states a tremendous function of our spinal cord neurons. The human spinal cord receives senses of touch from different locations in different parts of it. Multiple vertebrae can be connected to one internal organ too. Fig. 1(a) presents simplified rough connections between human touch-sensors and the spinal cord. Researchers have developed convolutional neural networks (CNN) by mimicking the functionality of the cats' visual cortex and that brings a significant improvement in the accuracy of NNs [6]. The wonderful spinal architecture and the recent success of CNNs

motivate us to develop a neural network with gradual inputs.

A well-known approach to reducing computation is pooling [7]. However, pooling causes loss of information. Popular solutions to the vanishing gradient problem are ResNet and DenseNet. They allow shortcut connections over different layers. Therefore, the gradient remains high at neurons near the input [8]. ResNets always provide better performance with increasing depth and can be as deep as thousands of layers. However, the marginal improvement of ResNet is very low. The depth needs to be doubled for a percentage improvement in the performance. Moreover, very deep ResNets have a problem of diminishing feature reuse. Therefore, Sergey et al. proposed wide residual networks [9] and achieved superior performance. Zifeng et al. also received superior performance with shallow and wide NNs [10]. Gao et al. propose DenseNet where all layers are connected [11]. DenseNet training is faster and provides better performance in most situations due to two reasons 1) all layers of DenseNet are connected, 2) they made dense-net narrower than the ResNet. When all layers are connected, the gradient and feature-reuse do not vanish over layers. However, as all layers are connected, an increment of the network-size by one layer needs connections to that layer from all existing layers. Therefore, deep DenseNets are computation extensive. Adaptive Structural Learning of Neural Networks(AdaNet) performs both connecting neurons and optimizing weights during the training. Consideration of all possible connections of a DNN is computationally intensive. The inauguration of a new neuron requires the consideration of connecting the neuron to all existing neurons. Therefore, AdaNet is suitable for shallow neural networks (NNs) [12], [13].

Existing DNNs have vanishing gradient problem and there exists a high order increase in the number of connections with an increased number of layers. Existing DNNs cannot be narrowed down to a few neurons when the number of input is large. This paper proposes the SpinalNet, presented as figure 1(b) to overcome these issues. The proposed structure with gradual and repetitive input capabilities enables the NNs to be very deep. Moreover, we investigate the proposed SpinalNet as the fully connected layer of CNNs and receive better performance most of the situation.

II. THEORETICAL BACKGROUND

Deep NNs can be convolutional or non-convolutional. Non-convolutional NNs consists of inputs, hidden layers, and outputs, shortly fully connected layers. Deep CNNs contain convolutional layers and fully-connected layers. The convolution increases the number of parameters significantly. Pooling is applied to reduce the number of parameters [14]. Vogt [15] believes that there are two main points to the importance of pooling in deep learning methods. Firstly, pooling declines the size of input for the next layer but it allows learning more mappings. Second, pooling assists in combining the output obtained from the prior layer on a large scale. However, pooling also causes the loss of information, as it considers only the maximum or average of nearby values [15], [16]. Pooled information is converted to a one-dimensional vector through

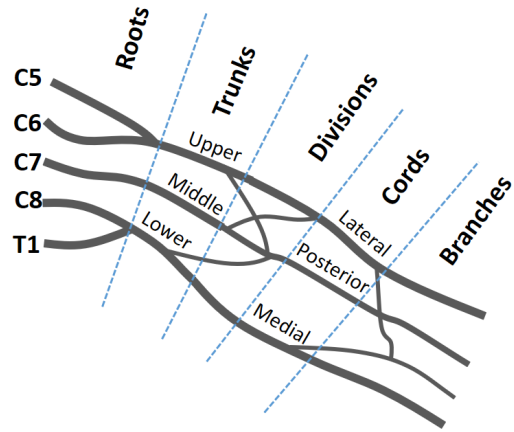


Fig. 2. A portion of the human nerve plexus, known as brachial plexus. The information of any touch or pain reaches the brain through the nerve plexus and the spinal cord. Nerve plexus is a network of intersecting nerves. Our spinal cord receives information gradually. Here, C5-C8 and T1 are vertebrae in the human skeleton [19].

flattening. Finally, fully-connected layers compute the output from the one-dimensional vector.

A. Human Somatosensory System and the Spinal Cord

Although the exact mechanism of the human Somatosensory system is not well understood, we find several similarities between the human spinal cord and the proposed neural network [17]. Features we tried to mimic are as follows:

- 1) Gradual input and nerve plexus
- 2) Voluntary and involuntary actions
- 3) Attention to pain intensity

Sensory neurons reach the spinal cord through a complex network, known as nerve plexus. Fig. 2 presents a portion of nerve plexus. Single vertebrae do not receive all the information. The tactile sensory network consists of millions of sensors. Moreover, our tactile system is more stable compared to the vision or the auditory system, as there is a much fewer number of 'touch-blind' patients than the number of blindness. The nerve plexus network sends all tactile signals to the spinal cord gradually. Different locations of a spinal cord receive the pain of leg and the pain of hand [17]. Neurons in vertebrae transfer the sense of touch to the brain and may take some actions. Our brain can control the spinal neurons, to increase or decrease the pain intensity [18]. Sensory neurons may also convey information to the lower-motor before getting instruction from the brain. That is called involuntary movements, or reflex movements.

B. Proposed SpinalNet

The proposed SpinalNet has the following similarities with the abovementioned features of the human spinal cord.

- 1) Gradual input
- 2) Local output and probable global influence
- 3) Weights reconfigured during training

Similar to our spinal cord, the proposed SpinalNet takes inputs gradually. Inputs are provided gradually and repetitively. Each

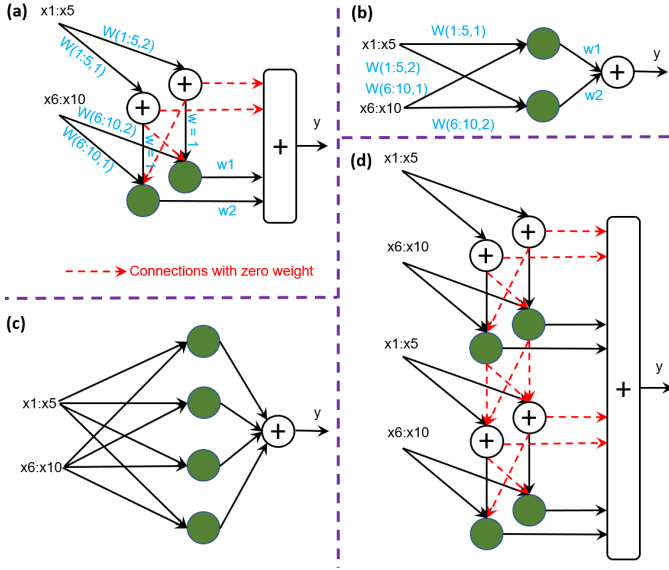


Fig. 3. The visual proof of the universal approximation theorem for the proposed SpinalNet. A simplified version of SpinalNet in (a) can act as a NN of a single hidden layer, drawn in (b). Similarly, a 4 layer SpinalNet in (d) can be equal to a NN of one hidden layer (HL), containing four neurons, shown in (c).

layer of the SpinalNet contributes towards the local output (reflex). The SpinalNet also sends a modulated portion of input towards the global output (brain). NN training configures weights based on the training data and our brain configures the spinal neurons for tuning the pain sensitivity for different sensories of our skin.

Fig. 1(b) presents the structure of the proposed SpinalNet. The network structure consists of an input row, an intermediate row, and an output row. The input is split and sent to the intermediate row of multiple hidden layers. In Fig. 1(b), the intermediate row, and the output row contain two neurons per hidden layer. The number of output neurons per hidden layer is equal to the number of outputs. The number of intermediate neurons can be changed according to the user. However, both the number of intermediate neurons and the number of inputs per layer is usually kept small to reduce the number of multiplication. As the number of inputs and the number of intermediate hidden neurons per layer is usually low, the network may underfit. Therefore, each layer receives inputs from the previous layer. As the input is repeated, if one important feature of input does not impact on the output in one hidden layer, the feature may impact the output in another hidden layer. The intermediate row contains nonlinear activation function and the output row contains linear activation function. In Fig. 1(b), input values are split into three rows. Rows are assigned to different hidden layers repeatedly.

C. Universal Approximation of the Proposed SpinalNet

Whenever a new neural network structure is proposed, there raises a question about its universal approximability. Therefore, the universal approximation is proved for many recent popular neural networks [20], [21]. The traditional mathematical proof of the universal approximation theorem

contains scholarly and esoteric equations. However, we aim to make the paper equation-free to attract the general audience. Therefore, we prove the universal approximation with the following approach.

- 1) Single hidden layer NN of large width is a universal approximator [22].
- 2) If we can prove that, SpinalNet of a large depth can be equivalent to the single hidden layer NN of large width, the universal approximation is proved.

Fig. 3 presents how a simpler version of SpinalNet can be converted to a single hidden layer NN. In Fig. 3(a), a SpinalNet of 2 hidden layers (HLs), each layer containing 2 neurons is simplified. The neurons of the first layer are simplified to the purely linear function. Therefore the first layer takes only the weighted sum of x_1 to x_5 inputs. Outputs of each hidden neuron of the first hidden layer only go to a similar neuron of the second hidden layer. Cross connections and connections from the first hidden layer to output are disconnected by assigning zero weight. The second hidden layer receives the weighted sum of x_6 to x_{10} . It also receives the weighted sum of x_1 to x_5 from the previous layer. Therefore, neurons of this layer apply an activation function to the weighted sum of x_1 to x_{10} . Therefore, these two layers are equivalent to a neural network of single HL, containing two hidden neurons, shown in Fig. 3(b). A simplified version of SpinalNet of 4HL, containing 2 neurons in each layer is shown in Fig. 3(d). Similarly, that SpinalNet is also equivalent to a NN of one HL, containing 4 neurons.

Similarly, a SpinalNet of large depth can be equivalent to a NN of a single hidden layer, containing a large number of neurons. A NN of a single hidden layer, containing a large number of neurons achieves the universal approximation. Therefore, a SpinalNet of large depth also achieves the universal approximation.

III. RESULTS

This paper verifies the effectiveness of the SpinalNet for regression and classification problems. We have shown comparable performance with SpinalNet in regression. Popular classification problems are classifying MNIST datasets and the CIFAR datasets. Several publicly available codes for these datasets are downloaded and executed. All of the standard codes and SpinalNet codes apply the gradient descent technique for NN training. As the dataset and codes are publicly available, future researchers may easily compare results.

A. Regression Dataset

Regression is a less popular topic among the researchers of NN compared to classification. There exist a large number of datasets and organized competition among various algorithms for the classification problem. Therefore, we compare our SpinalNet with the PyTorch regression example, developed by Ben Phillips [23]. The example considers a single input and a single output. The example applies the Adam algorithm [24] to optimize. The loss function is the Mean-square-error (MSE), the learning rate is 0.01, and the number of the epoch is 200. We changed the problem to 8-variable and

TABLE I
COMPARISON BETWEEN TRADITIONAL FEED-FORWARD NN AND
SPINALNET FOR REGRESSION

Neural Network	Data	MSE (10^{-3} Unit)	
		100 Epoch	200 Epoch
Feed-forward NN Two Hidden Layers 200, 100 Neurons [23]	8 Var. $\sum x$	1.178	0.887
	8 Var. $\sin(\sum x)$	1.918	1.086
	8 Var. $\prod x$	3.875	3.875
	8 Var. $\sin(\prod x)$	3.403	1.554
SpinalNet 6 Hidden Layers 50 Neurons Each Layer Half Input Each Layer	8 Var. $\sum x$	1.007	0.855
	8 Var. $\sin(\sum x)$	1.912	1.219
	8 Var. $\prod x$	3.966	2.217
	8 Var. $\sin(\prod x)$	0.910	0.910

tried with different combinations of variables with the same level of noise. Combinations are 1) summation of variables ($\sum x$), 2) sine of summation of variables ($\sin(\sum x)$), 3) product of variables ($\prod x$), and 4) sine of product of variables ($\sin(\prod x)$). We record the MSE at 100 and 200 epochs. The default code [23] shows MSE of the last epoch, but our code shows the minimum MSE of the current and previous epochs. The input is segmented into two segments, containing four inputs each.

The number of hidden neurons in traditional NN is 300 [23]. The number of hidden neurons in SpinalNet is also 300. The number of multiplication in traditional NN is 21700, and the number of multiplications in SpinalNet is 14000. The SpinalNet achieves a 35.5% reduction in the number of multiplications. There are 8-combinations for MSE comparisons, as shown in Table I. Superior performances are highlighted as bold characters. The SpinalNet performs better in six out of eight combinations.

B. Classification Datasets

We train several existing networks and different variations of SpinalNet on MNIST, Fashion-MNIST, KMNIST, QMNIST, EMNIST, CIFAR-10, and CIFAR-100 classification data sets.

1) *MNIST*: The MNIST dataset is the most popular datasets for investigating image classification algorithms due to its simplicity. The default fully-connected layer of the PyTorch CNN example has 320 parameters after flattening [25]. A hidden layer of fifty neurons joins them with the output. The default code provides 98.17% accuracy. We investigate the same NN with a SpinalNet fully-connected(FC) layer. The FC layer consists of six sub-hidden layers, each layer contains eight neurons. That CNN with Spinal FC provides 98.44% accuracy. That structure brings more than a 48.5% reduction in multiplication and a 4% reduction in the activation functions on the fully-connected layer.

Another Spinal FC structure contains six sub-hidden layers, each layer contains ten neurons. That CNN(Spinal FC) provides 98.48% accuracy. That structure brings more than a 35% reduction in multiplication but a 20% increase happens in the activation functions on the fully-connected layer. To achieve a higher accuracy we consider another NN architecture (SpinalNet(Arch2)), containing three SpinalNets. The architecture is depicted in Fig. 4 Initial parameters, parameters after the first convolution, and parameters after the second convolution are flattened and three SpinalNet are applied to

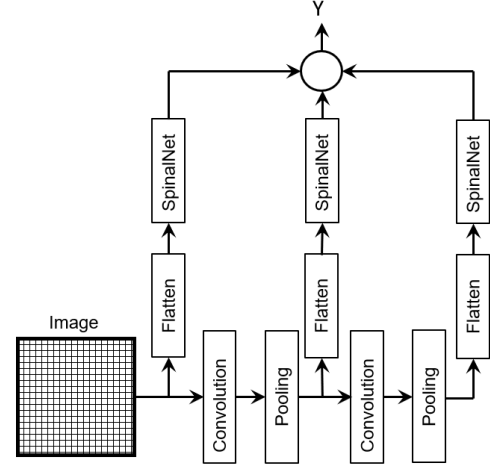


Fig. 4. Structure of the second architecture (Arch2) of the SpinalNet. This structure receives flattened outputs of the original image, images after the first convolution & pooling, and images after second convolution & pooling.

three flattened data. The first SpinalNet consists of 10 spinal layers, where the other two SpinalNet consists of 8 spinal layers. The width of each spinal layer is 30. That structure (SpinalNet(Arch2)) brings 99.61% accuracy. Although the complexity of the network is increased, we receive a significant reduction in error. According to our knowledge, it is one of the top 20 reported performance on the MNIST dataset. We also apply the random perspective and the random rotation functions to achieve that performance. The random rotation function is applied with the ten-degree angle.

As VGG models perform very well with the MNIST datasets, we incorporate the SpinalNet with the VGG-5 network [26]. VGG-5 with the Spinal fully connected layer provides a near state-of-the-art performance. We receive 99.72% accuracy with VGG-5(Spinal FC). The data augmentation on the MNIST dataset for SpinalNet(Arch2), VGG-5, and VGG-5(Spinal FC) are the same.

2) *Fashion-MNIST*: The Fashion-MNIST data is quite similar to MNIST. It also contains 28×28 grayscale images and the output contains 10 classes. Therefore, MNIST codes can exactly be applied to the Fashion-MNIST data. The same NN is applied to compute CNN and CNN(Spinal FC). Applying the random perspective does not improve the performance of NNs on the Fashion-MNIST data. The SpinalNet(Arch2) structure is the same but the random perspective is not applied. The random rotations of 10 degrees are applied and contain 300 neurons in each hidden layer. The performance is 92.74%. According to our knowledge, our accuracy on the Fashion-MNIST data is one of the top ten reported results.

We receive 94.68% accuracy with VGG-5(Spinal FC). The data augmentation on the Fashion-MNIST dataset for SpinalNet(Arch2), VGG-5, and VGG-5(Spinal FC) are the same. The default VGG-5 provides 94.63% accuracy. Therefore, the Spinal FC provides better performance with a lower number of multiplications.

3) *Kuzushiji-MNIST*: Kuzushiji-MNIST or shortly, KMNIST is a Japanese character recognition dataset. The data format of KMNIST is also the same as the MNIST data

and the same codes can be applied. Table II presents the performance of codes. The Arch2 provides 97.22% accuracy. As it a comparatively new dataset, there exist very few reported works. Our accuracy on KMNIST data is one of the top ten reported results.

We receive 99.15% accuracy with VGG-5(Spinal FC). The data augmentation on the MNIST dataset for SpinalNet(Arch2), VGG-5, and VGG-5(Spinal FC) are the same. The default VGG-5 provides 98.94% accuracy. Therefore, the Spinal FC provides better performance with a lower number of multiplications.

4) *QMNIST*: QMNIST is a recently published English digit recognition dataset. QMNIST has fifty thousand test images. The dimensions of inputs and outputs are the same as the dimension of inputs and outputs of the MNIST dataset. Therefore, the same code can be executed for the QMNIST dataset. The results are presented in table II. The default PyTorch CNN provides 97.82% accuracy on the QMNIST data. CNN(Spinal FC) provides 97.97%-98.07% accuracy and SpinalNet(Arch2) provides 99.36% accuracy. As it is new data there exist a few reported results and our accuracy is one of the top 10 reported accuracies.

The VGG-5 receives 99.66% accuracy. The VGG-5(Spinal FC) receives 99.68% accuracy. According to our literature search, we have received state-of-the-art performance for the QMNIST dataset.

5) *EMNIST*: The EMNIST dataset contains several hand-written character datasets. These datasets are derived from the NIST Special Database 19 and converted to a 28×28 pixel image format. The data-type is the same and the EMNIST(digits) dataset has also 10 classes. Therefore, the same code can be executed for the EMNIST(digits) dataset. The accuracy of NNs on the EMNIST(digit) data are presented in table II. The default PyTorch CNN provides 98.89% accuracy and SpinalNet(Arch2) provides 99.65% accuracy.

The VGG-5 provides 99.81% accuracy and VGG-5(Spinal FC) provides 99.82% accuracy. According to our literature search, we have received state-of-the-art performance for the EMNIST(digits) dataset.

6) *CIFAR-10 Dataset*: The CIFAR-10 dataset is less predictable compared to the original MNIST dataset. The PyTorch CNN example [27] classifies the CIFAR-10 data with 60% accuracy. A SpinalNet of 6 hidden layers, each layer containing 20 neurons achieves 62% accuracy for the same number of epochs. 5% lower error is achieved with a 4.8% multiplication reduction at the fully-connected layer.

The DenseNet code [28] shared by Hasan et al. provides 77.79% accuracy after 35 epochs. The DenseNet fully connected layer has a 512 neuron hidden layer. We train a SpinalNet of 8 hidden layers, each containing 16 neurons. The number of hidden neurons becomes one-fourth and the number of multiplication is reduced by 87%. Still, we observe a 15% error reduction. Another SpinalNet has 8 hidden layers, each containing 64 neurons. The number of hidden neurons remains the same and the number of multiplication is reduced by 44.1%. The error is reduced by 18.7% compared to the previous DenseNet code [28].

The ResNet [29] example of PyTorch provides 88.35% accuracy after 80 cycles. We achieve 88.65% accuracy after 80 cycles and 88.93% accuracy after 140 cycles with a SpinalNet of 4 hidden layers, each layer contains 16 neurons. However, we reduce the pooling and increase multiplication at the fully-connected layer at the default ResNet code [29]. However, the accuracy is lower with the standard ResNet blocks. The spinal fully-connected layer degrades the performance of ResNet-18 and ResNet-34 slightly.

A consistent improvement in the NN size and performance is achieved with the VGG network. As the VGG neural network contains a large fully-connected layer, the SpinalNet can act as an optimized fully-connected layer. We investigate VGG-11, VGG-13, VGG-16, and VGG-19. VGG-19 provides the highest accuracy (91.40%) among VGG networks and VGG SpinalNets. However, the ResNet-18 provides 91.98% accuracy, and adding a Spinal fully connected layer degrades the accuracy.

According to our results, the SpinalNet brings significant improvement on NNs, containing activation functions in the fully connected layer. ResNet has no activation on the fully connected layer. Therefore, the improvement of ResNet with a SpinalNet FC layer is not significant. Therefore, we consider a dropout CNN, containing a large number of activation function on the fully connected layer [30]. The dropout CNN provides 87.29% accuracy where the consideration of the SpinalNet fully-connected layer brings 89.08% accuracy.

7) *CIFAR-100 Dataset*: As dropout CNN, ResNet, and VGG networks bring promising results with CIFAR-10 data, we apply them on the CIFAR-100 dataset. We receive significant improvement with the Spinal fully-connected layer for dropout CNN and different VGG networks. Among VGG networks, VGG-16 provides the best performance. VGG-16 provides 63.20% accuracy alone, and 64.99% accuracy with the SpinalNet after 150 epoch of training. Moreover, the number of neurons in the fully connected layer is reduced to half with the Spinal fully-connected layer. Moreover, the number of multiplication in the fully-connected layer is reduced to 7%.

The dropout CNN network is trained for 35 epoch and the performance is improved from 50.29% to 57.33%. However, the Spinal fully-connected layer does not improve the performance of ResNet. Although the number of hidden neurons in the fully connected layer is increasing for ResNet, we are getting a lower performance. The probable reason can be a decrease in the gradient in the initial layers of ResNet due to additional layers.

C. The Highest Accuracy

The state of the art (SOTA) performances for different datasets are presented as table III. Combining SpinalNet with VGG-5 provides near SOTA or SOTA performance in MNIST datasets. Models performing SOTA performance are usually a combined model and have the best performance for a specific dataset. We also succeeded to obtain SOTA performance for the EMNIST (digits) dataset. However, the prime reason for obtaining SOTA is not the proposed network. As the dataset is new, very few researchers investigated this data and our result is the best among the reported results.

TABLE II
PERFORMANCE OF THE SPINALNET AND SEVERAL POPULAR NETS ON DIFFERENT DATASETS

Data	Model	Size of Fully Connected Layer	Epoch	Test Accuracy	Error Reduction
MNIST [31]	CNN [25]	1HL, 50 Neurons	8	98.17%	-
	CNN(Spinal FC)	6HL, 8 Neurons Per Layer	8	98.44%	14.8%
	CNN(Spinal FC)	6HL, 10 Neurons Per Layer	8	98.48%	16.9%
	SpinalNet(Arch2)	*	120	99.61%	78.7%
	VGG-5 [26]	1HL, 512 Neurons	100	99.72%	-
Fashion-MNIST [32]	VGG-5(Spinal FC)	4HL, 128 Neurons Per Layer	100	99.72%	0.0%
	CNN [25]	1HL, 50 Neurons	8	84.10%	-
	CNN(Spinal FC)	6HL, 8 Neurons Per Layer	8	85.98%	11.8%
	CNN(Spinal FC)	6HL, 10 Neurons Per Layer	8	86.61%	15.8%
	SpinalNet(Arch2)	*	200	92.74%	54.3%
Kuzushiji-MNIST (KMNIST) [33]	VGG-5 [26]	1HL, 512 Neurons	100	94.63%	-
	VGG-5(Spinal FC)	4HL, 128 Neurons Per Layer	100	94.68%	0.9%
	CNN [25]	1HL, 50 Neurons	8	84.48%	-
	CNN(Spinal FC)	6HL, 8 Neurons Per Layer	8	87.94%	22.3%
	CNN(Spinal FC)	6HL, 10 Neurons Per Layer	8	88.25%	24.3%
QMNIST [34]	SpinalNet(Arch2)	*	160	97.22%	82.1%
	VGG-5 [26]	1HL, 512 Neurons	200	98.94%	-
	VGG-5(Spinal FC)	4HL, 128 Neurons Per Layer	200	99.15%	19.8%
	CNN [25]	1HL, 50 Neurons	8	97.82%	-
	CNN(Spinal FC)	6HL, 8 Neurons Per Layer	8	97.97%	6.9%
EMNIST (Digits) [35]	CNN(Spinal FC)	6HL, 10 Neurons Per Layer	8	98.07%	11.5%
	SpinalNet(Arch2)	*	100	99.36%	70.6%
	VGG-5 [26]	1HL, 512 Neurons	100	99.66%	-
	VGG-5(Spinal FC)	4HL, 128 Neurons Per Layer	100	99.68%	5.9%
	CNN [25]	1HL, 50 Neurons	8	98.89%	-
CIFAR-10 [36]	CNN(Spinal FC)	6HL, 8 Neurons Per Layer	8	99.12%	20.7%
	CNN(Spinal FC)	6HL, 10 Neurons Per Layer	8	99.16%	24.3%
	SpinalNet(Arch2)	*	55	99.65%	68.5%
	VGG-5 [26]	1HL, 512 Neurons	50	99.81%	-
	VGG-5(Spinal FC)	4HL, 128 Neurons Per Layer	50	99.82%	5.3%
	CNN [27]	2HL, 120 and 84 Neurons	8	60.65%	-
	CNN(Spinal FC)	6HL, 20 Neurons Per Layer	8	62.37%	4.4%
	DenseNet [28]	1HL, 512 Neurons	35	77.79%	-
	DenseNet(Spinal FC)	8HL, 16 Neurons Per Layer	35	81.13%	15.0%
	DenseNet(Spinal FC)	8HL, 64 Neurons Per Layer	35	81.95%	18.7%
	ResNet [29]	Only Output Layer	80	88.35%	-
	ResNet(Spinal FC)	4HL, 16 Neurons Per Layer	80	88.65%	2.6%
	ResNet(Spinal FC)	4HL, 16 Neurons Per Layer	140	88.93%	5.0%
	ResNet-18 [8]	Only Output Layer	150	91.98%	-
	ResNet-18(Spinal FC)	4HL, 20 Neurons Per Layer	150	91.42%	-7.0%
	ResNet-34 [8]	Only Output Layer	150	89.56%	-
	ResNet-34(Spinal FC)	4HL, 256 Neurons Per Layer	150	89.88%	3.1%
	CNN-Dropout [30]	2HL, 1024 and 512 Neurons	50	87.29%	-
	CNN-Dropout(Spinal FC)	4HL, 50 Neurons Per Layer	31	89.08%	14.1%
	CNN-Dropout(Spinal FC)	4HL, 128 Neurons Per Layer	160	90.83%	27.9%
VGG-11 [37]	2HL, 4096 Neurons Each	35	86.68%	-	
VGG-11(Spinal FC)	4HL, 1024 Neurons Each	35	87.08%	3.0%	
VGG-13 [37]	2HL, 4096 Neurons Each	35	87.79%	-	
VGG-13(Spinal FC)	4HL, 1024 Neurons Each	35	89.16%	11.2%	
VGG-19 [37]	2HL, 4096 Neurons Each	200	90.75%	-	
VGG-19(Spinal FC)	4HL, 512 Neurons Each	200	91.40%	7.0%	
CIFAR-100 [36]	CNN-Dropout [30]	2HL, 1024 and 512 Neurons	35	50.29%	-
	CNN-Dropout(Spinal FC)	4HL, 128 Neurons Per Layer	35	57.33%	14.2%
	ResNet-18 [8]	Only Output Layer	30	65.04%	-
	ResNet-18(Spinal FC)	4HL, 128 Neurons Per Layer	30	63.60%	-4.1%
	ResNet-34 [8]	Only Output Layer	30	65.51%	-
	ResNet-34(Spinal FC)	4HL, 128 Neurons Per Layer	30	63.32%	-6.3%
	VGG-11 [37]	2HL, 4096 Neurons Each	40	55.60%	-
	VGG-11(Spinal FC)	4HL, 1024 Neurons Each	40	60.48%	11.0%
	VGG-13 [37]	2HL, 4096 Neurons Each	50	60.75%	-
	VGG-13(Spinal FC)	4HL, 1024 Neurons Each	50	62.46%	4.4%
	VGG-16 [37]	2HL, 4096 Neurons Each	150	63.20%	-
	VGG-16(Spinal FC)	4HL, 512 Neurons Each	150	64.99%	4.9%
	VGG-19 [37]	2HL, 4096 Neurons Each	150	62.05%	-
	VGG-19(Spinal FC)	4HL, 512 Neurons Each	150	64.77%	7.2%

* Fig. 4 presents the structure of SpinalNet(Arch2), the second architecture. The SpinalNet(Arch2) consists of three SpinalNets.

The later section presents how we can replace each hidden layer of a conventional NN with a SpinalNet layer. In the future, we may incorporate the proposed SpinalNet with SOTA models to obtain the best performance for more datasets.

IV. PROSPECTS OF SPINALNET

This paper is the very first paper on the SpinalNet. In the future, researchers may find many improvements.

A. Auto Dimension Reduction

Dimension reduction is a popular technique of reducing the number of inputs to a neural network without facing noticeable performance degradation [44]. The input combination of the NN network may contain a large number of inter-related data, irrelevant data and constants. As the proposed SpinalNet takes input in every layer and there are fewer neurons per hidden layer than the total number of inputs, the SpinalNet may automatically discard irrelevant and excess data. Moreover, the necessity for dimension reduction may decrease, as a large number of input features do not increase computation greatly.

B. Transfer Learning

Although the number of hidden neurons in the fully connected layer is increasing, the ResNet with Spinal FC is getting a lower performance compared to the similar ResNet. The probable reason can be a decrease in the gradient in the initial layers of ResNet due to additional layers. Therefore, in the future, we may apply the transfer learning technique to the pre-trained ResNet. The pre-trained ResNet can be the initial layers of a ResNet, providing one of the best performance on the same dataset.

C. Very Deep NN

The computation inside the proposed SpinalNet increases linearly with the increase in depth. ResNet also has the same advantage but the ResNet faces the vanishing gradient problem a much higher depth. The SpinalNet has outputs at every layer. Moreover, gradual training may enable SpinalNet trainer to increase the network depth gradually.

D. Spinal Hidden Layer

This paper presents the SpinalNet as an independent network and as the fully connected layer of a CNN. The SpinalNet can also replace a wide hidden layer of a traditional NN. Fig. 5 presents how a SpinalNet can replace a traditional hidden layer. The figure shows two inputs and one neuron per sub-layer. The number of inputs can be large and the input can be segmented into more than two segments. Similarly, one sub-layer may hold more than one neuron. The number of sub-layer can be more than or less than four.

E. Better Accuracy and New Datasets

The SpinalNet may achieve higher accuracy with augmented datasets and different structural variants. Such as, in SpinalNet(Arch2) we apply three SpinalNet to achieve high accuracy. Researchers may apply SpinalNet for different datasets, new applications [45]–[47], and combining with other networks in the future.

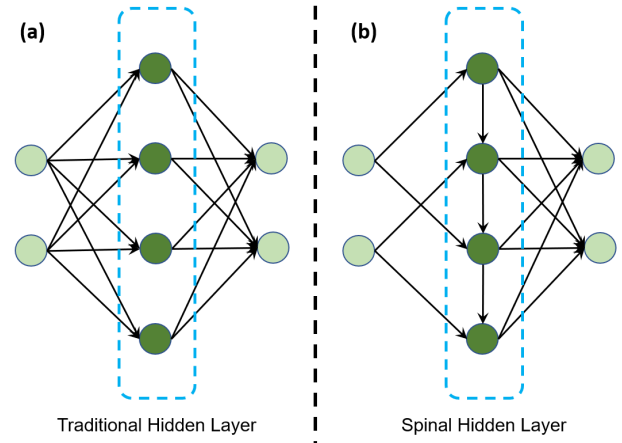


Fig. 5. Any traditional hidden layer can be converted to a spinal hidden layer. The traditional hidden layer in (a) is converted to a spinal hidden layer in (b). A spinal hidden layer has the structure of the proposed SpinalNet.

F. NN Ensemble and Voting

Recently Mo Kweon et al. perform ensemble and voting from two different VGG networks and ResNet to achieve better performance [26]. Researchers may use different NN along with SpinalNet to get better performance.

V. CONCLUSION

This paper aims to present the concept and structure of the SpinalNet. The chordate nervous system has a unique way of connecting large numbers of sensing information and taking local decisions. A drawback of recent DNNs is computation intensiveness due to a large number of inputs. Therefore, taking inputs gradually and considering local decisions like our spinal cord decreases computations. The paper also presents the effectiveness of SpinalNet on MNIST and CIFAR-10 dataset. The SpinalNet improves the accuracy of classification. Moreover, the SpinalNet is usually less computation extensive than its counterpart. In the future, we will try to improve accuracies and apply SpinalNet to new fields.

REFERENCES

- [1] A. Byerly, T. Kalganova, and I. Dear, "A branching and merging convolutional network with homogeneous filter capsules," *arXiv preprint arXiv:2001.09136*, 2020.
- [2] D. Ciregan, U. Meier, and J. Schmidhuber, "Multi-column deep neural networks for image classification," in *2012 IEEE conference on computer vision and pattern recognition*. IEEE, 2012, pp. 3642–3649.
- [3] Y. Bengio, A. Courville, and P. Vincent, "Representation learning: A review and new perspectives," *IEEE transactions on pattern analysis and machine intelligence*, vol. 35, no. 8, pp. 1798–1828, 2013.
- [4] K. Kowsari, M. Heidarysafa, D. E. Brown, K. J. Meimandi, and L. E. Barnes, "Rmdl: Random multimodel deep learning for classification," in *Proceedings of the 2nd International Conference on Information System and Data Mining*, 2018, pp. 19–28.
- [5] S. Okamoto, H. Nagano, and Y. Yamada, "Psychophysical dimensions of tactile perception of textures," *IEEE Transactions on Haptics*, vol. 6, no. 1, pp. 81–93, 2012.
- [6] D. H. Hubel and T. N. Wiesel, "Receptive fields, binocular interaction and functional architecture in the cat's visual cortex," *The Journal of physiology*, vol. 160, no. 1, pp. 106–154, 1962.
- [7] S. Lawrence, C. L. Giles, A. C. Tsoi, and A. D. Back, "Face recognition: A convolutional neural-network approach," *IEEE transactions on neural networks*, vol. 8, no. 1, pp. 98–113, 1997.

TABLE III
SOTA PERFORMANCE IN JUNE 2020*

Data	Model Name	Reference	Accuracy	Error
MNIST	Branching/Merging CNN + Homogeneous Filter Capsules	[1]	99.84%	0.16%
Fashion-MNIST	PreAct-ResNet18 + FMix	[38]	96.36%	3.64%
Kuzushiji-MNIST**	VGG8B	[39]	99.01%	0.99%
QMNISt**	Deep Regularization	[40]	99.67%	0.33%
EMNIST (Digits)**	DWT-DCT with KNN	[41]	97.74%	2.26%
CIFAR-10	GPIPE + transfer learning	[42]	99.00%	1.00%
CIFAR-100	BiT-L (ResNet)	[43]	93.51%	6.49%

* According to the following website: www.paperswithcode.com/task/image-classification and our literature search.

** After the online appearance of the current paper, the performance of SpinalNet will be SOTA. Unless someone reports a better performance earlier.

- [8] K. He, X. Zhang, S. Ren, and J. Sun, "Deep residual learning for image recognition," in *Proceedings of the IEEE conference on computer vision and pattern recognition*, 2016, pp. 770–778.
- [9] S. Zagoruyko and N. Komodakis, "Wide residual networks," *arXiv preprint arXiv:1605.07146*, 2016.
- [10] Z. Wu, C. Shen, and A. Van Den Hengel, "Wider or deeper: Revisiting the resnet model for visual recognition," *Pattern Recognition*, vol. 90, pp. 119–133, 2019.
- [11] G. Huang, Z. Liu, L. Van Der Maaten, and K. Q. Weinberger, "Densely connected convolutional networks," in *Proceedings of the IEEE conference on computer vision and pattern recognition*, 2017, pp. 4700–4708.
- [12] C. Cortes, X. Gonzalvo, V. Kuznetsov, M. Mohri, and S. Yang, "Adanet: Adaptive structural learning of artificial neural networks," in *Proceedings of the 34th International Conference on Machine Learning-Volume 70*. JMLR. org, 2017, pp. 874–883.
- [13] H. D. Kabir, A. Khosravi, and S. Nahavandi, "Partial adversarial training for neural network-based uncertainty quantification," *IEEE Transactions on Emerging Topics in Computational Intelligence*, 2019.
- [14] T. Wiatowski and H. Bölcskei, "A mathematical theory of deep convolutional neural networks for feature extraction," *IEEE Transactions on Information Theory*, vol. 64, no. 3, pp. 1845–1866, 2017.
- [15] M. Vogt, "An overview of deep learning and its applications," in *Fahrerassistenzsysteme 2018*. Springer, 2019, pp. 178–202.
- [16] L. Xie, Q. Tian, and B. Zhang, "Simple techniques make sense: Feature pooling and normalization for image classification," *IEEE transactions on circuits and systems for video technology*, vol. 26, no. 7, pp. 1251–1264, 2015.
- [17] R. D'mello and A. Dickenson, "Spinal cord mechanisms of pain," *British journal of anaesthesia*, vol. 101, no. 1, pp. 8–16, 2008.
- [18] C. Sprenger, F. Eippert, J. Finsterbusch, U. Bingel, M. Rose, and C. Büchel, "Attention modulates spinal cord responses to pain," *Current Biology*, vol. 22, no. 11, pp. 1019–1022, 2012.
- [19] T. N.-J. Chang, K.-T. Chen, T. Gorden, B. W. Daniel, C. Hernon, M. Shafarenko, Y.-L. Huang, J. C.-Y. Lu, and D. C.-C. Chuang, "Vascularized brachial plexus allotransplantation experimental study in brown norway and lewis rats," *Transplantation*, vol. 103, no. 1, pp. 149–159, 2019.
- [20] H. Lin and S. Jegelka, "Resnet with one-neuron hidden layers is a universal approximator," in *Advances in neural information processing systems*, 2018, pp. 6169–6178.
- [21] F. Fan, J. Xiong, and G. Wang, "Universal approximation with quadratic deep networks," *Neural Networks*, vol. 124, pp. 383–392, 2020.
- [22] B. C. Csáji *et al.*, "Approximation with artificial neural networks."
- [23] B. Phillips, "Regression with neural networks in pytorch." [Online]. Available: <https://medium.com/@benjamin.phillips22/simple-regression-with-neural-networks-in-pytorch-313f06910379>
- [24] D. P. Kingma and J. Ba, "Adam: A method for stochastic optimization," *arXiv preprint arXiv:1412.6980*, 2014.
- [25] G. Koehler, "Mnist handwritten digit recognition in pytorch." [Online]. Available: nextjournal.com/gkoehler/pytorch-mnist
- [26] M. Kweon, "Mnist competition tensorflow kr group." [Online]. Available: <https://github.com/kkweon/mnist-competition>
- [27] PyTorch, "Training a classifier." [Online]. Available: pytorch.org/tutorials/beginner/blitz/cifar10_tutorial.html
- [28] S. M. K. Hasan, "Densenet implementation on cifar10 dataset using pytorch." [Online]. Available: <https://github.com/SMKamrulHasan/DenseNet-using-PyTorch-CIFAR10>
- [29] PyTorch, "3.2.2 resnet_cifar10-pytorch tutorial." [Online]. Available: https://pytorch-tutorial.readthedocs.io/en/latest/tutorial/chapter03_intermediate/3_2_2_cnn_resnet_cifar10/
- [30] Z. Na, "Deep learning with pytorch on cifar10 dataset." [Online]. Available: <https://zhenye-na.github.io/2018/09/28/pytorch-cnn-cifar10.html>
- [31] L. Deng, "The mnist database of handwritten digit images for machine learning research [best of the web]," *IEEE Signal Processing Magazine*, vol. 29, no. 6, pp. 141–142, 2012.
- [32] H. Xiao, K. Rasul, and R. Vollgraf, "Fashion-mnist: a novel image dataset for benchmarking machine learning algorithms," *arXiv preprint arXiv:1708.07747*, 2017.
- [33] T. Clanuwat, M. Bober-Irizar, A. Kitamoto, A. Lamb, K. Yamamoto, and D. Ha, "Deep learning for classical japanese literature," *arXiv preprint arXiv:1812.01718*, 2018.
- [34] C. Yadav and L. Bottou, "Cold case: The lost mnist digits," in *Advances in Neural Information Processing Systems*, 2019, pp. 13 443–13 452.
- [35] G. Cohen, S. Afshar, J. Tapson, and A. Van Schaik, "Emnist: Extending mnist to handwritten letters," in *2017 International Joint Conference on Neural Networks (IJCNN)*. IEEE, 2017, pp. 2921–2926.
- [36] A. Krizhevsky, G. Hinton *et al.*, "Learning multiple layers of features from tiny images," 2009.
- [37] K. Simonyan and A. Zisserman, "Very deep convolutional networks for large-scale image recognition," *arXiv preprint arXiv:1409.1556*, 2014.
- [38] E. Harris, A. Marcu, M. Painter, M. Niranjan, A. Prügel-Bennett, and J. Hare, "Understanding and enhancing mixed sample data augmentation," *arXiv preprint arXiv:2002.12047*, 2020.
- [39] A. Nøkland and L. H. Eidnes, "Training neural networks with local error signals," *arXiv preprint arXiv:1901.06656*, 2019.
- [40] G. R. Yoo and H. Owahdi, "Deep regularization and direct training of the inner layers of neural networks with kernel flows," *arXiv preprint arXiv:2002.08335*, 2020.
- [41] P. Ghadekar, S. Ingole, and D. Sonone, "Handwritten digit and letter recognition using hybrid dwt-dct with knn and svm classifier," in *2018 Fourth International Conference on Computing Communication Control and Automation (ICCCUBEA)*. IEEE, 2018, pp. 1–6.
- [42] Y. Huang, Y. Cheng, A. Bapna, O. Firat, D. Chen, M. Chen, H. Lee, J. Ngiam, Q. V. Le, Y. Wu *et al.*, "Gpipe: Efficient training of giant neural networks using pipeline parallelism," in *Advances in neural information processing systems*, 2019, pp. 103–112.
- [43] A. Kolesnikov, L. Beyer, X. Zhai, J. Puigcerver, J. Yung, S. Gelly, and N. Houlsby, "Large scale learning of general visual representations for transfer," *arXiv preprint arXiv:1912.11370*, 2019.
- [44] M. Vohra, A. Alexanderian, H. Guy, and S. Mahadevan, "Active subspace-based dimension reduction for chemical kinetics applications with epistemic uncertainty," *Combustion and Flame*, vol. 204, pp. 152–161, 2019.
- [45] H. D. Kabir, A. Khosravi, M. A. Hosen, and S. Nahavandi, "Neural network-based uncertainty quantification: A survey of methodologies and applications," *IEEE Access*, 2018.
- [46] S. Rahman, S. Khan, and F. Porikli, "A unified approach for conventional zero-shot, generalized zero-shot, and few-shot learning," *IEEE Transactions on Image Processing*, vol. 27, no. 11, pp. 5652–5667, 2018.
- [47] D. Neven, B. De Brabandere, S. Georgoulis, M. Proesmans, and L. Van Gool, "Towards end-to-end lane detection: an instance segmentation approach," in *2018 IEEE intelligent vehicles symposium (IV)*. IEEE, 2018, pp. 286–291.